Available online at www.sciencedirect.com
SCIENCE DIRECT®
Biochimica et Biophysica Acta 1655 (2004) 306–320
BIOCHIMICA ET BIOPHYSICA ACTA
BBA
www.bba-direct.com

Review

Active site structure of the aa_3 quinol oxidase of *Acidianus ambivalens*

Tapan Kanti Das[a,b], Cláudio M. Gomes[c,d], Tiago M. Bandeiras[c], Manuela M. Pereira[c], Miguel Teixeira[c], Denis L. Rousseau[a,*]

[a] *Department of Physiology and Biophysics, Albert Einstein College of Medicine, 1300 Morris Park Avenue, Bronx, NY 10461, USA*
[b] *Pfizer Inc., 700 Chesterfield Parkway, Chesterfield, MO 63017, USA*
[c] *Instituto de Tecnologia Quimica e Biológica, Universidade Nova de Lisboa, APT 127, 2780-156 Oeiras, Portugal*
[d] *Faculdade de Ciências e Tecnologia, Universidade Nova de Lisboa, Monte da Caparica, Portugal*

Received 6 May 2003; received in revised form 24 July 2003; accepted 1 August 2003

Abstract

The membrane bound aa_3-type quinol:oxygen oxidoreductase from the hyperthermophilic archaeon, *Acidianus ambivalens*, which thrives at a pH of 2.5 and a temperature of 80 °C, has several unique structural and functional features as compared to the other members of the heme–copper oxygen reductase superfamily, but shares the common redox-coupled, proton-pumping function. To better understand the properties of the heme a_3–Cu_B catalytic site, a resonance Raman spectroscopic study of the enzyme under a variety of conditions and in the presence of various ligands was carried out. Assignments of several heme vibrational modes as well as iron–ligand stretching modes are made to serve as a basis for comparing the structure of the enzyme to that of other oxygen reductases. The CO-bound oxidase has conformations that are similar to those of other oxygen reductases. However, the addition of CO to the resting enzyme does not generate a mixed valence species as in the bovine aa_3 enzyme. The cyanide complex of the oxidized enzyme of *A. ambivalens* does not display the high stability of its bovine counterpart, and a redox titration demonstrates that there is an extensive heme–heme interaction reflected in the midpoint potentials of the cyanide adduct. The *A. ambivalens* oxygen reductase is very stable under acidic conditions, but it undergoes an earlier alkaline transition than the bovine enzyme. The *A. ambivalens* enzyme exhibits a redox-linked reversible conformational transition in the heme a_3–Cu_B center. The pH dependence and H/D exchange demonstrate that the conformational transition is associated with proton movements involving a group or groups with a pK_a of $\sim$ 3.8. The observed reversibility and involvement of protons in the redox-coupled conformational transition support the proton translocation model presented earlier. The implications of such conformational changes are discussed in relation to general redox-coupled proton pumping mechanisms in the heme–copper oxygen reductases.

Keywords: Raman spectroscopy; Bioenergetics; Midpoint potential; Heme proteins; Proton translocation

1. Introduction

Studies of heme–copper oxygen reductases originating from phylogenetically distant microorganisms contribute significantly both to a wider knowledge of the functional, structural, and mechanistic diversity found among prokaryotic oxygen reductases, and to a better understanding of the common features of this enzyme superfamily. An example of a heme–copper oxygen reductase with quite distinct features is the Type B [1,2] aa_3 quinol oxidase from the thermoacidophilic archaeon *Acidianus ambivalens* [3–5]. This organism grows optimally at 80 °C and pH 2.5 [6,7], and contains one of the simplest respiratory systems so far described. The essential structural elements of the enzyme are the same as those of the other members of the heme–copper oxygen reductase family, containing a heme *a* redox center and a heme a_3–Cu_B binuclear catalytic site where oxygen is reduced to water.

Functional and mechanistic studies on the *A. ambivalens* aa_3 quinol oxidase have revealed several distinct properties of this enzyme in comparison to its mitochondrial counterpart, especially in the dynamics of the heme a_3–Cu_B binuclear center [8,9]. Moreover, in spite of the absence of the conserved amino acid residues of the D-channel identified for the other heme–copper oxygen reductases, it was shown to be a proton pump [5]. Investigations by stopped-flow spectrophotometry sug-

* Corresponding author. Tel.: +1-718-430-4264/3591; fax: +1-718-430-8808/4230.
E-mail address: rousseau@aecom.yu.edu (D.L. Rousseau).

0005-2728/$ - see front matter © 2004 Elsevier B.V. All rights reserved.
doi:10.1016/j.bbabio.2003.08.011

gested that the enzyme interacts in vivo with a redox active molecule, most probably caldariella quinone, which favors the electron entry via heme *a*, providing the fourth electron demanded for catalysis [4]. The quinone is essentially lost upon purification of the enzyme. This situation finds a parallel in *Escherichia coli* bo_3 quinol oxidase, which also requires the presence of a tightly bound quinone to have normal oxygen reaction kinetics [10]. Additional data from independent experimental approaches have been accumulating and suggest an intrinsic difference of the *A. ambivalens* quinol oxidase binuclear site with respect to that of the other enzymes in this superfamily. In this oxidase, in the detergent solubilized form, the apparent reduction potential for heme a_3 is higher than that of heme *a* [4], in contrast with what is observed with the canonical oxygen reductases, which have a reversed order. In agreement with the redox potential data, no electron back flow is observed from heme a_3 to heme *a* upon photolysis of the mixed valence CO-bound enzyme [9]. Also, the ligand binding properties of the *A. ambivalens* reductase, judged by the reaction with CO, are quite different from those of the other oxygen reductases. CO-recombination kinetics data demonstrate that CO binds transiently to Cu_B before binding to heme a_3 just as in the bovine enzyme, but at much lower rates, the overall process being slower by a factor of ~ 25. Additionally, in the *A. ambivalens* oxygen reductase, distinct absorbance changes in the visible region in the tens of microsecond time scale have been tentatively ascribed as a heme a_3 pocket relaxation that occurs on the same time scale as that of the CO release from the Cu_B site [9]. These changes are significantly slower than those reported for the bovine enzyme. The role of such conformational changes in the binuclear center associated with ligand binding/dissociation events have not been delineated in the proton pumping mechanism but clearly have potential importance.

The bound quinone in the *A. ambivalens* aa_3 enzyme also plays a role in the regulation of the dynamics of the binuclear site. Resonance Raman spectroscopy showed that a change in frequency of the heme a_3 formyl group, from 1660 to 1667 cm^{-1}—indicative of a loss of hydrogen bonding due to deprotonation of a neighboring group—is influenced by the presence of quinone [8]. The conformational change associated with this shift is reversible and it occurs faster in the presence of caldariella quinone. Therefore, the quinone brings about changes, which lead to a structural modification at the binuclear site upon reduction, a process with implications on proton translocation [8].

Pereira et al. [1] have classified the heme–copper oxygen reductases into three different types depending on their proton pathways. *A. ambivalens* aa_3 belongs to Type B in which the amino acid residues in the D and K channels are not conserved, as they are in Type A, although an alternative K channel homologue seems to be present. (In the Type C oxygen reductases, the D channel is absent and an alternative K channel is only partly conserved.) All three types have been shown to act as proton pumps [1]. In these enzymes, two distinct functional processes involve protons. Four protons are utilized in the dioxygen reduction process to generate two molecules of water; these protons are taken up from the matrix side of the inner mitochondrial membrane in eukaryotes, or from the cytoplasmic side in prokaryotes. In addition, up to four protons are pumped from the matrix (or cytoplasm) to the other side of the membrane for each oxygen molecule reduced. The coupling of the electron/chemical events to the proton movements imposes the existence of redox-sensitive protonation sites in the enzyme [8,11–16], which must undergo protonation/deprotonation events associated with the catalytic and electron transfer events and may lead to key rearrangements of hydrogen bonding networks, including water molecules (e.g., see Refs. [1,2]). During proton translocation, conformational changes may also be required, to assure the vectoriality of the process. In the *A. ambivalens* enzyme, the redox-linked conformational changes in the heme a_3–Cu_B site, as noted above, have been ascribed as constituting a crucial element in the proton translocation mechanism [8].

We report here a structural characterization of this enzyme using resonance Raman spectroscopic methods as well as measurements of the heme midpoint potentials to study its ligand binding and heme pocket properties. The features of this enzyme are highlighted in comparison to those of bovine aa_3 in an effort to identify those properties that are similar and those that are distinct.

2. Materials and methods

2.1. Materials

A. ambivalens cells were grown as described elsewhere [17]. Membranes and purified aa_3 oxygen reductase were prepared as in Ref. [5], using *n*-dodecyl-β-D-maltoside as detergent. The concentration of the protein samples used for the Raman measurements was ~ 60 μM in appropriate buffer for a desired pH (100 mM sodium phosphate, pH 7.4 and pH 2.6; 100 mM sodium acetate, pH 3.5–5.0; 100 mM MES, pH 6.0; 100 mM CHES, pH 9.0–9.5; 100 mM CAPS, pH 10.5). Decylubiquinone and dodecyl maltoside were purchased from Sigma (St. Louis, MO).

2.2. Methods

Resonance Raman measurements were carried out with excitation wavelengths at 413.1 nm from a Krypton-Ion laser (Spectra Physics, Mountain View, CA) and 441.7 nm from a He–Cd laser (Liconix, Santa Clara, CA). Details of the instrumentation have been described elsewhere [18]. The sample cell was spun at 6000 rpm to avoid local heating.

The Raman scattered light was dispersed through a polychromator (Spex, Metuchen, NJ) equipped with a 1200 grooves/mm grating and detected by a liquid nitrogen-cooled CCD camera (Princeton Instruments, Princeton, NJ). A holographic notch filter (Kaiser, Ann Arbor, MI) was used to remove the laser scattering. Frequency shifts in the Raman spectra were calibrated using acetone–CCl_4 or indene as a reference.

In the Raman measurements, the membrane fraction (containing exclusively the aa_3 oxidase) was studied in the intact state and in the solubilized state by the addition of detergent. The purified enzyme lacks bound quinone, as determined from quinone extraction and HPLC analyses, which consistently showed the absence of caldariella quinone. The purified enzyme yielded a good signal-to-noise level in the Raman measurements as compared to the intact membrane preparation. To obtain the reduced samples, an aliquot of a freshly prepared anaerobic solution of dithionite was added to a degassed solution of the oxidized enzyme. Owing to sensitivity of the oxidized enzyme (except at very low or high pH), low laser power ($\sim$ 0.1–0.5 mW depending on the duration of data acquisition) was used in the resonance Raman measurements. For the same reason, low power was used for the CO complex as well as for the cyanide-bound oxidized enzyme. To measure the spectrum of the photodissociated CO sample, the laser beam, at relatively high power ($\sim$ 20 mW), was tightly focused on the spinning Raman cell, such that the passage time of the sample through the beam was $\sim$ 5 μs. Assuming that the first half of the passage of the sample through the beam resulted in complete photodissociation, the photoproduct has an effective evolution time of $\sim$ 2 μs. Additional experimental details for each measurement are given in the figure legends. All measurements were carried out at ambient temperature except otherwise noted. The Raman measurements were carried out with a custom made quartz cell that is also suitable for UV–Vis absorption measurements. The samples were sealed in the cell, and UV–Vis spectra recorded before and after Raman measurements to check the stability of the species studied.

The anaerobic redox titration of *A. ambivalens* oxygen reductase ($\sim$ 1.8 μM) was performed as previously described [19]. To form the cyanide adduct, the enzyme was incubated overnight with 10 mM of cyanide, at 4 °C, pH 7.5, in complete darkness. The redox mediators (2.4 μM each) used were the following: *N*,*N*-dimethyl-*p*-phenylenediamine (E_0'=+340 mV), *p*-benzoquinone (E_0'=+240 mV), 1,2-naphtoquinone-4-sulfonic acid (E_0'=+215 mV), trimethylhydroquinone (E_0'=+115 mV), phenazine methosulfate (E_0'=+80 mV), 1,4-naphtoquinone (E_0'=+60 mV), phenazine ethosulfate (E_0'=+55 mV), duroquinone (E_0'=+5 mV). The pH of the mixture was verified before and after the titration. The data shown is the result of two independent titrations. The potentials are quoted in relation to the standard hydrogen electrode.

3. Results

3.1. Resonance Raman spectra

The high-frequency region (1300–1700 cm^{-1}) of the resonance Raman spectra of hemeproteins are comprised of porphyrin in-plane vibrational modes that are sensitive to the electron density in the porphyrin macrocycle and also to the oxidation, coordination, and spin state of the central iron atom [20]. In addition, the C–O stretching mode of the heme-substituent formyl groups and the C–C stretching mode of heme-substituent vinyl groups are present in the high-frequency region [21]. In the respiratory oxygen reductases containing heme *a* as a redox cofactor, the carbonyl stretching mode from the formyl group of both heme *a* and heme a_3 are resonance-enhanced and are located in the 1600–1700 cm^{-1} region. As such, they are useful probes of the local environment of the heme periphery. Fig. 1 shows the resonance Raman spectra in the high-frequency region of the purified *A. ambivalens* aa_3 oxygen reductase in the as-isolated oxidized and dithionite-reduced forms of the enzyme. Also shown is the spectrum of the enzyme in the intact membrane of *A. ambivalens*. For tentative mode assignments, see Table 1 in which the spectral lines from *A. ambivalens* aa_3 are compared to those of the bovine enzyme [22–24]. The characteristics of the modes of the heme macrocycle are similar to those seen in other oxidases but the carbonyl modes of the formyl group are quite distinct.

3.2. Resonance Raman spectra of the oxidized enzyme

The spectrum of the enzyme in the as-isolated oxidized form (Fig. 1c) has vibrational modes from both hemes *a* and a_3, resembling those in bovine oxidase (Table 1). The C–O stretching modes of the formyl groups are assigned at 1653 and 1676 cm^{-1}, for heme *a* and heme a_3, respectively. The C–O formyl mode at 1676 cm^{-1} from heme a_3 in the *A. ambivalens* oxidase is located at a higher frequency than that (1672 cm^{-1}) in the bovine enzyme [21], suggesting a less polar (or weaker hydrogen bonding) character in vicinity of the formyl C=O moiety in the *A. ambivalens* oxygen reductase. The C–O formyl mode of heme *a* is also found at higher frequency (by 11 cm^{-1}) than that in the bovine enzyme (Table 1), suggesting a significant difference in the electrostatic environment of heme *a* between the two enzymes in the oxidized state. The quality of the spectra in the oxidized forms of the enzyme is not as good as that of the reduced forms of the enzyme (see below) due to the high photosensitivity of the heme groups in this enzyme, which necessitates use of low laser power to avoid photodissociation. Great care was taken to minimize photoreduction by using low laser power and spinning the sample cells.

The carbonyl mode of the heme a_3 formyl group in the oxidized form of *A. ambivalens* oxidase undergoes changes in its frequency in the presence of ubiquinone. It is known that the *A. ambivalens* aa_3 oxidase binds ubiquinone leading

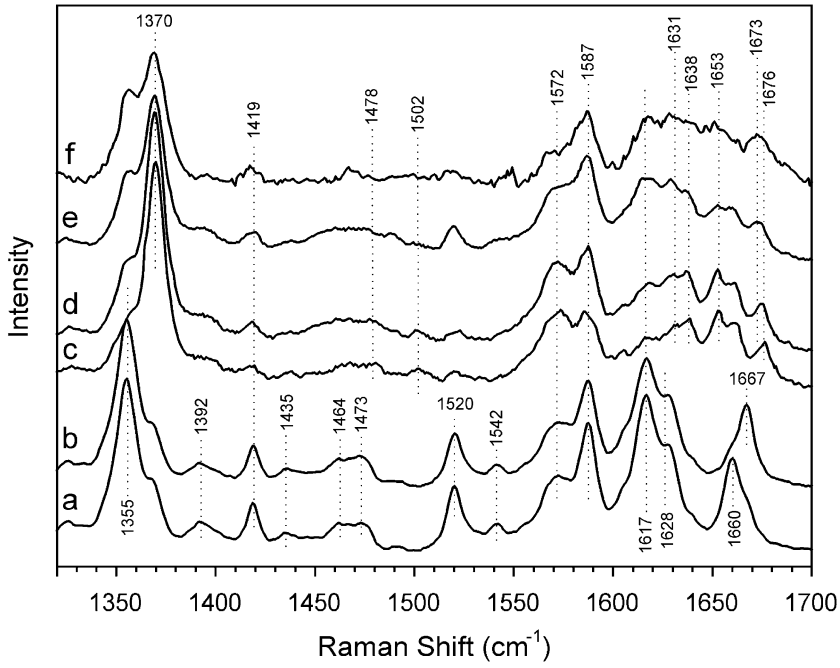

Fig. 1. Resonance Raman spectra of oxidized and reduced *A. ambivalens* aa_3 oxygen reductase in the high-frequency region showing the formyl stretching frequency as functions of time and decylubiquinone addition. The enzyme (60 μM) was reduced anaerobically by dithionite, in 100 mM MES and 1 mg/ml dodecyl maltoside at pH 6. The spectra of reduced enzyme shown are (a) immediately (~ 1 min) and (b) 50 min after reduction. The spectra of the oxidized enzyme (as-purified, ~ 60 μM, 100 mM sodium phosphate, pH 7.4) shown are (c) with no added decyl ubiquinol, (d) with 1.1 mM decyl ubiquinol, incubated for 15 min, (e) with a large excess (5.5 mM) of decyl ubiquinol, incubated for 15 min. The spectrum of the whole membrane in the oxidized (as-isolated, pH 7) form is also shown in (f). The excitation frequency was 413.1 nm. The data acquisition time with the oxidized samples was about 1 min, the laser power used was ~ 0.5 mW, and the sample cell was spun at 6000 rpm. These were found to be the optimum conditions to minimize photoreduction while achieving an acceptable quality of spectra. The laser power for reduced samples was ~ 20 mW.

to altered electron transfer activity in the enzyme [4,8]. The carbonyl stretching mode of the formyl group shifts to lower frequency (1673 cm^{-1}) in the presence of decylubiquinone (Fig. 1d,e), suggesting a more polar environment around the heme a_3 formyl moiety. The spectrum of the membrane enzyme (Fig. 1f) supports such an effect of quinone binding

Table 1
Selected heme vibrational modes of hemes *a* and a_3 from *A. ambivalens* oxygen reductase in the oxidized (Oxid) and reduced (Red) states in comparison to the corresponding modes of bovine heart aa_3[a]

Mode	*A. ambivalens* aa_3					Bovine aa_3				
	Oxid	Oxid CN^-	Red	Red CN^-	Red CO	Oxid	Oxid CN^-	Red	Red CN^-	Red CO
$\nu_{C=O,\ formyl}\ a_3$	1676	1674	1667	1654	1667	1672	1671	1664	1644	1666
	1673 (mem)		1661 (transient)							
$\nu_{C=O,\ formyl}\ a$	1653	1653	1628	1629	1629	1642	1642	1611	1611	1611
$\nu_{C=C,\ vinyl}$	1620	1624	1617	1619	1618	1620	1620	1622	1625	1618
ν_{10}	1638	1640	1638	–	–	1637	–	1608	–	–
$\nu_2\ a_3$	1572	–	1572	–	–	1569	–	1567	–	–
$\nu_2\ a$	1587	1588	1587	1588	1588	1582	1586	1583	1585	1585
ν_{37}	1572	1573	1572	1572	1572	1568	1570	1567	1567	1567
$\nu_{11}\ a^{+2}$	–	–	1520	1520	1520	–	–	1518	1520	1516
$\nu_3\ a_3$	1478	1502	1473	1492	1500	1476	–	1466	–	–
$\nu_3\ a$	1502	1502	1492	1492	1492	1503	–	1493	–	–
ν_{28}	1467	1467	1464	1465	1465	–	–	1464	–	1469
ν_4	1370	1371	1355	1357	1357 (*a*)	1368	1369	1355	1356	1355 (*a*)
					1367 (a_3)					1368 (a_3)
ν_{16}	751	–	747	–	750	755	–	747	745	747
ν_7	681	–	680	–	684	683	–	686	680	683
ν_{Fe-CO}	–	–	–	–	520, 500	–	–	–	–	520
ν_{C-O}					1970					1964
δ_{Fe-C-O}					567					578
$\nu_{Fe-His}(a_3^{+2})$	–	–	210	–	–	–	–	213	–	–

[a] The bovine data was obtained from Refs. [22–24].

because the intact membrane-bound enzyme has its physiological partner, caldariella quinone, bound to it, and the frequency of the formyl mode is centered at 1673 cm^{-1} in the oxidized form.

3.3. Reduction of the enzyme

Immediately following anaerobic reduction of the enzyme, the frequencies of the vibrational modes in the Raman spectrum (Fig. 1a) have some similarities to those in other oxygen reductases and some significant differences (see Table 1 for comparison with the bovine enzyme). The formyl carbonyl stretching modes are assigned at 1628 and 1660 cm^{-1}, for heme *a* and heme a_3, respectively [8], immediately after reduction of the enzyme. Our assignment of the carbonyl stretching mode of the heme *a* formyl mode at 1628 cm^{-1} places it nearly 20 cm^{-1} higher than that in the bovine enzyme [21] although substantially lower than that of the mode in *Sulfolobus acidocaldarius* in which it was assigned at 1657 cm^{-1} [25]. The assignment of the formyl mode of heme *a* at 1628 cm^{-1} was based on the correlation of the intensity of this line with the amount of reduced heme *a*. The other possibility for this mode is the line at $\sim$ 1621 cm^{-1}. However, in comparison with the other members of the a_3–Cu_B superfamily, it appears more likely that the 1621 cm^{-1} line results from the vinyl C=C stretching mode.[1] The higher frequency of the formyl mode in the enzyme from *A. ambivalens* as compared to that from the bovine enzyme indicates that the hydrogen bonding to the formyl group is substantially weaker in the *A. ambivalens* aa_3.

The heme a_3 formyl mode initially detected at 1660 cm^{-1} shows a time-dependent change following reduction, shifting to 1667 cm^{-1} (Fig. 1b). The absence of spectral changes in the other modes, including the oxidation state marker, ν_4, at 1355 cm^{-1}, indicates that the oxidation, coordination, and spin states are not changing in either of the hemes as a function of time after reduction. As reported previously [8], this redox-induced conformational change in heme a_3 of the purified enzyme is slow with a $t_{1/2}$ $\sim$ 18 min. In the membrane-bound enzyme, however, the conformational changes occur much faster.

To probe further into the redox-induced conformational changes, the effect of proton/deuterium (H/D) exchange in the enzyme was followed. In these experiments, pairs of samples were prepared under identical conditions except that one was incubated in H_2O buffer and the other in D_2O buffer. The sample pairs were followed as a function of time after reduction. Shown in Fig. 2 are spectra at three time intervals (spectra in bold lines are for the H_2O samples and those in thin lines are for the D_2O samples). Although initially, the spectra are very similar with respect to the 1660 cm^{-1} conformer population, the transition to the 1667 cm^{-1} conformer is much slower in D_2O relative to that in H_2O. Even after prolonged time (80 min), when the conformational transition is complete in H_2O, the D_2O sample retains some 1660 cm^{-1} population. Thus, the redox-induced transition is retarded by the proton to deuterium exchange. These observations demonstrate that the conformational transition involving the heme a_3 formyl group is associated with proton movements, which may include changes in the hydrogen bonding network close to the binuclear site.

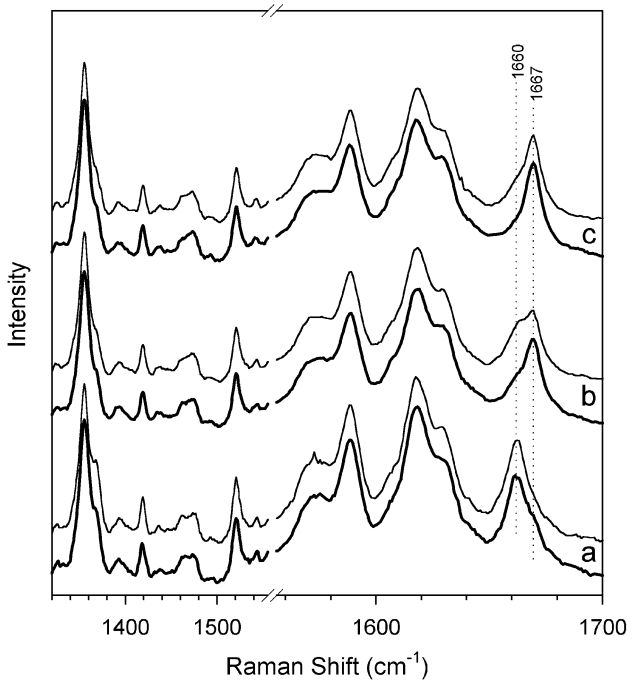

Fig. 2. The effect of H/D exchange on the redox-mediated change in the formyl mode frequency in *A. ambivalens* aa_3 oxygen reductase. Reduction-induced (anaerobically by dithionite) changes in the spectra in H_2O (bold line) and in D_2O (thin line) were followed as a function of time. The spectra shown are at (a) immediately following reduction, at $\sim$ 1 min, (b) after 40 min, and (c) after 80 min. The excitation frequency was 413.1 nm and laser power on samples was $\sim$ 20 mW.

Additional insights into the conformational transition were obtained by examining the effects of pH and temperature on the conformational transition. The transition involves one (or more) proton exchangeable group with a p*K* of $\sim$ 3.8 [8]. The extent of the conversion from the 1660 to the 1667 cm^{-1} conformer depends on the medium pH (and on elapsed time following reduction, as discussed earlier). By raising the temperature of the reaction medium to 55 °C, the conformational transition is accelerated significantly (data not shown). For example, at pH 5, the conformational transition is complete in less than a minute at 55 °C, in comparison to tens of minutes at room temperature. A series of experiments were designed to study the reversibility of the conformational transition process as well as its dependence on protonation/deprotonation states of the involved groups. The reduction reaction in various pH buffers was carried out at 55 °C, and the reduced samples were incubated until equilibrium was reached. Then, the samples were taken out of the 55 °C bath

[1] In our prior report (see Ref. [8]), this same assignment was presented in the text but the figure in that paper (Fig. 1) listed the incorrect assignment.

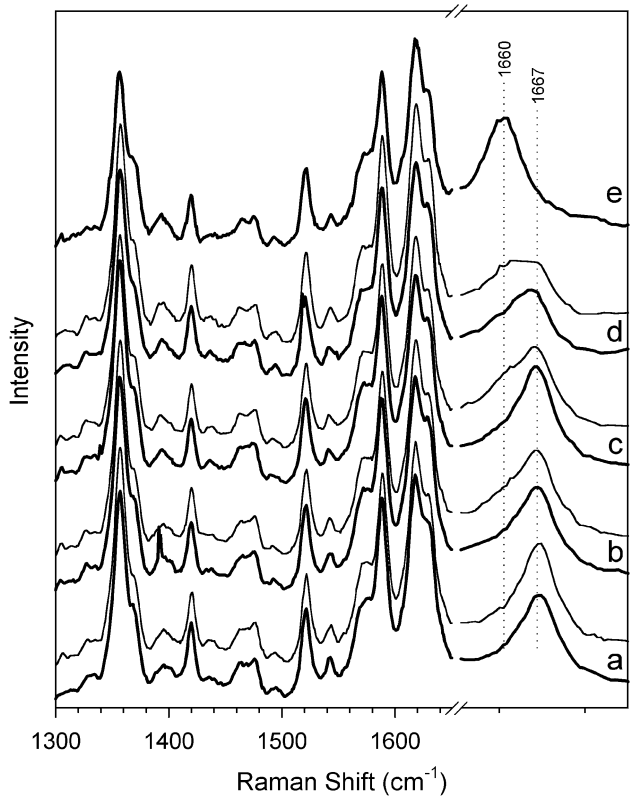

Fig. 3. The transition between the two conformers of the formyl group in *A. ambivalens* aa_3 oxygen reductase as functions of temperature and pH. The samples were incubated at 55 °C in a water bath for 10 min, followed by anaerobic dithionite reduction, and then incubation at 55 °C for another 10 min. Then the samples were placed at room temperature, and time-dependent resonance Raman spectra were recorded. Spectra shown are immediately after moving from 55 °C to room temperature (bold line), and after a sufficiently long time to reach equilibrium, 80 min (thin line); at pH 5 (a), pH 4.4 (b), pH 4 (c), pH 3.5 (c), and pH 2.6 (d). It may be noted that at pH 2.6, no conversion to the 1667 cm^{-1} form was observed even with incubation at 55 °C. At higher pH values, a pH-dependent recovery of the 1660 cm^{-1} conformer was seen. The excitation frequency was 413.1 nm and laser power on samples was ~ 20 mW.

and allowed to cool to room temperature, while monitoring their spectra to determine the population of the two conformers. Fig. 3 shows spectra of various pH samples at two time points: immediately after removing them from the 55 °C bath (shown in bold) and at equilibrium after sufficiently long time (80 min, shown in thin line). For the sample at pH 2.6, only one spectrum is shown because even after incubating at 55 °C, no conversion to the 1667 cm^{-1} conformer was observed. In the pairs of spectra from a through d at decreasing pH, the bold line spectra show a majority population of 1667 cm^{-1}, even at pH 3.5–4.0. However, in this pH range, cooling the samples to room temperature brings back a substantial population of the 1660 cm^{-1} conformer. These data indicate that as the temperature is increased, the pK_a is lowered. Based on the equal populations of the two species at pH 3.5, the pK_a change is ~ 0.3 pH units. In addition, the reversal of the populations upon lowering the temperature demonstrates the reversibility of the transition.

3.4. The cyanide-bound complexes

Cyanide binds to the iron of heme a_3 in both the oxidized and the reduced states of aa_3 oxygen reductases [24,26,27]. In the bovine enzyme, the cyanide binding to the oxidized heme a_3 is more stable than its binding in the reduced state. This is attributed to a very low midpoint potential of the cyanide adduct of heme a_3. Thus, a mixed valence species may be readily formed in which the heme *a* site is reduced and the CN-bound heme a_3 site is oxidized. This mixed valence form can be produced by reducing the cyanide adduct of the oxidized enzyme with limited amount of reductant or by simply exposing the fully reduced cyanide-bound form to oxygen [24].

Figs. 4 and 5 show the optical absorption spectra and the resonance Raman spectra for cyanide binding to various forms of *A. ambivalens* aa_3. When cyanide is added to the fully reduced form of the enzyme (Fig. 4a,b), the Soret band remains at 442 nm, and in the alpha region a component at

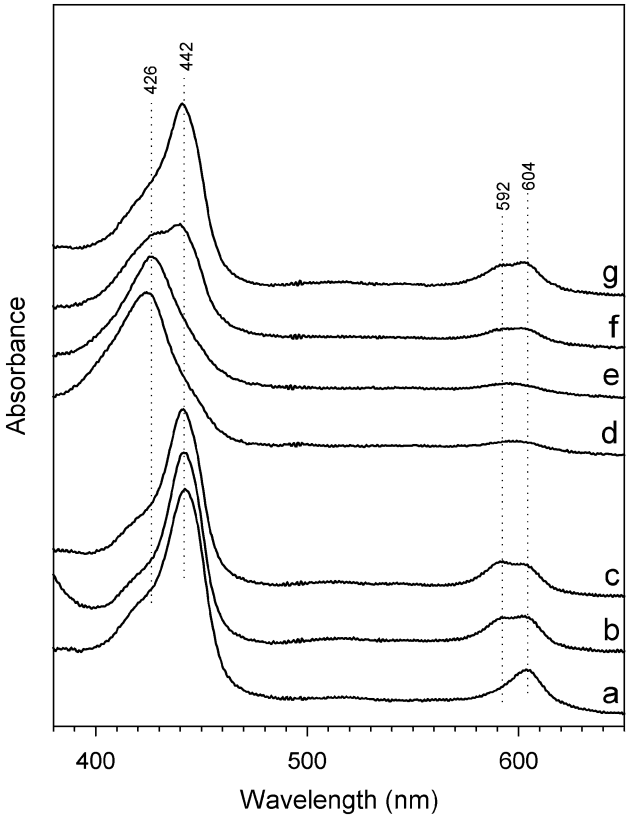

Fig. 4. UV–Visible absorption spectra of cyanide-bound *A. ambivalens* aa_3 oxygen reductase in the oxidized and reduced states at pH 7.4. Spectra shown are (a) fully reduced—absorption maxima at 442, 604 nm; (b) fully reduced, incubated with 10 mM cyanide for 100 minutes—absorption maxima at 442, ~ 592, ~ 604 nm; (c) reduced cyanide-bound enzyme in sample b after being exposed to air for 30 min. The following spectra were obtained from a different sample starting from the oxidized state of the enzyme: (d) as-isolated oxidized—absorption maxima at 424, 597 nm; (e) oxidized enzyme incubated with 10 mM cyanide; (f) the cyanide-bound enzyme from sample e was partially photoreduced using the 413.1 nm laser; (g) highly photoreduced cyanide-bound enzyme.

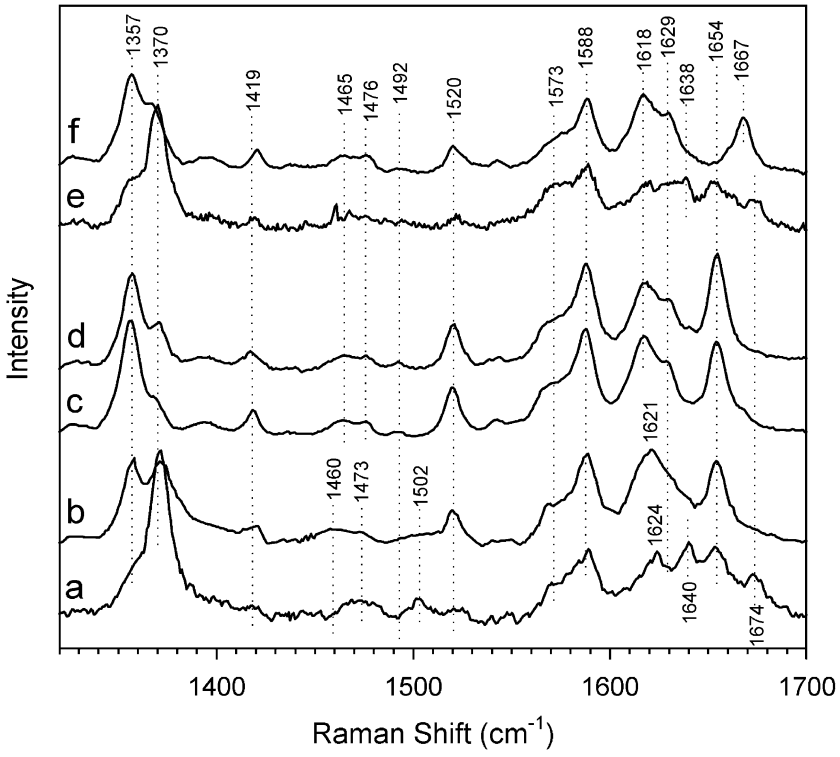

Fig. 5. Resonance Raman spectra of cyanide-bound *A. ambivalens* aa_3 oxygen reductase in oxidized and reduced states at pH 7.4 in the high-frequency region. Spectra shown are (a) as-isolated oxidized enzyme incubated with 10 mM cyanide; (b) photoreduction, using 413.1 nm beam, of cyanide-bound oxidized enzyme (sample a); (c) dithionite-reduced enzyme incubated with 10 mM cyanide under anaerobic condition; (d) reduced cyanide-bound enzyme from sample c left open in air overnight followed by the addition of a small amount of ferricyanide; (e) as-isolated oxidized enzyme incubated with CO in a sealed cell overnight; (f) fully reduced CO-bound enzyme. The excitation frequency was 413.1 nm, and laser power used on the sample was 0.1–2.0 mW.

592 nm develops, similar to the behavior seen in the fully reduced bovine enzyme [24]. The resonance Raman spectrum of the fully reduced cyanide-bound enzyme is characteristic of a low-spin reduced heme (Fig. 5, spectrum c) similar to that in the bovine enzyme. The frequencies of the modes that can be assigned to heme *a* are the same in the reduced CN^- adduct as in the reduced ligand-free and CO-bound species (see Table 1). Just as in the bovine enzyme, the heme a_3 formyl carbonyl stretching mode of the ferrous complex is lowered in frequency upon binding CN^-. However, the frequencies are quite different with the mode appearing at 1644 cm^{-1} in the bovine enzyme and at 1654 cm^{-1} in the *A. ambivalens* enzyme. When the cyanide-bound fully reduced form is exposed to air, which in the bovine enzyme yields a mixed-valence complex, the spectrum (spectrum c) is essentially unchanged (spectrum d).

Cyanide binding to the oxidized *A. ambivalens* enzyme results in a slight red shift (2 nm) of the Soret band (Fig. 4, spectra d and e). A larger red shift (5–12 nm, depending on the initial state of the enzyme—'fast' or 'slow', respectively [28,29]) upon cyanide binding is observed in the bovine enzyme, primarily because of a bluer Soret band of the oxidized form. Resonance Raman spectra of cyanide-bound *A. ambivalens* aa_3 in the oxidized state in the high-frequency region is shown in Fig. 5a. The cyanide-bound oxidized enzyme is very prone to photoreduction just as the oxidized enzyme itself, as noted above. Great care was taken to minimize such photoreduction as evident from the absence of intensity buildup at 1357 and 1520 cm^{-1} in spectrum a, which bears the signature of the low-spin, cyanide-bound oxidized aa_3 species ($\nu_4 = 1371$, $\nu_3 = 1502$, $\nu_2 = 1588$ cm^{-1}) (see Table 1). The formyl stretching frequencies of hemes a_3 and *a* appear at 1674 and 1653 cm^{-1}, respectively, very close to those in the oxidized enzyme in the absence of externally added cyanide, similar to observations made with the bovine enzyme (Table 1). The frequency of the carbonyl stretching mode of the heme *a* formyl group in the *A. ambivalens* enzyme of the CN^- adduct is the same as that in the absence of cyanide.

The cyanide-bound oxidized *A. ambivalens* enzyme is readily photoreduced as may be seen from the optical spectra in Fig. 4 (spectra f and g) just as the oxidized form in the absence of cyanide, described earlier. Spectrum g represents a highly photoreduced cyanide-bound species similar to the reduced cyanide-bound species shown in spectrum b, illustrating the propensity of the cyanide-bound species for photoreduction. Similar evidence for photoreduction comes from the resonance Raman spectrum when the laser power at 413.1 nm is increased. As may be seen from Fig. 5, spectrum b, both hemes *a* and a_3 become reduced. These results suggest that the midpoint potentials of the two hemes, when cyanide is bound, are similar in contrast to the bovine enzyme in

which the CN-bound heme a_3 has a very low potential. To determine quantitatively the redox behavior, a redox titration in the presence of 10 mM cyanide was performed. The enzyme spectra (from 350 to 800 nm) were measured as a function of the solution potential (Fig. 6). Surprisingly, the intensity changes in the Soret band (not shown) and at 592 and 604 nm follow almost exactly the same redox behavior (see Fig. 6, panel A), indicating that the two hemes have identical apparent midpoint potentials. Moreover, compared to the redox behavior of the cyanide-free enzyme (Fig. 6, panel A), it is immediately clear that the high redox potential transition is shifted to higher potential, by ca. 120 mV. At the present stage, a fitting of the experimental data was not attempted, due to the very large number of parameters necessary (intrinsic reduction potentials of each heme, heme–heme, and heme–copper interaction potentials). Nevertheless, it is clear that upon cyanide binding, the *A. ambivalens* enzyme shows an unexpected behavior, as compared with the bovine enzyme, namely an increase of the heme midpoint potentials.

3.5. Carbon-monoxide-bound conformers

The CO derivatives of hemeproteins are extremely useful probes for studying the environment of the heme proximity [22]. The frequencies of the Fe–CO stretching mode and other CO-related modes, which are particularly sensitive to interactions with neighboring groups, can be measured by resonance Raman spectroscopy. The frequencies of the Fe–CO stretching mode in the members of the heme–copper

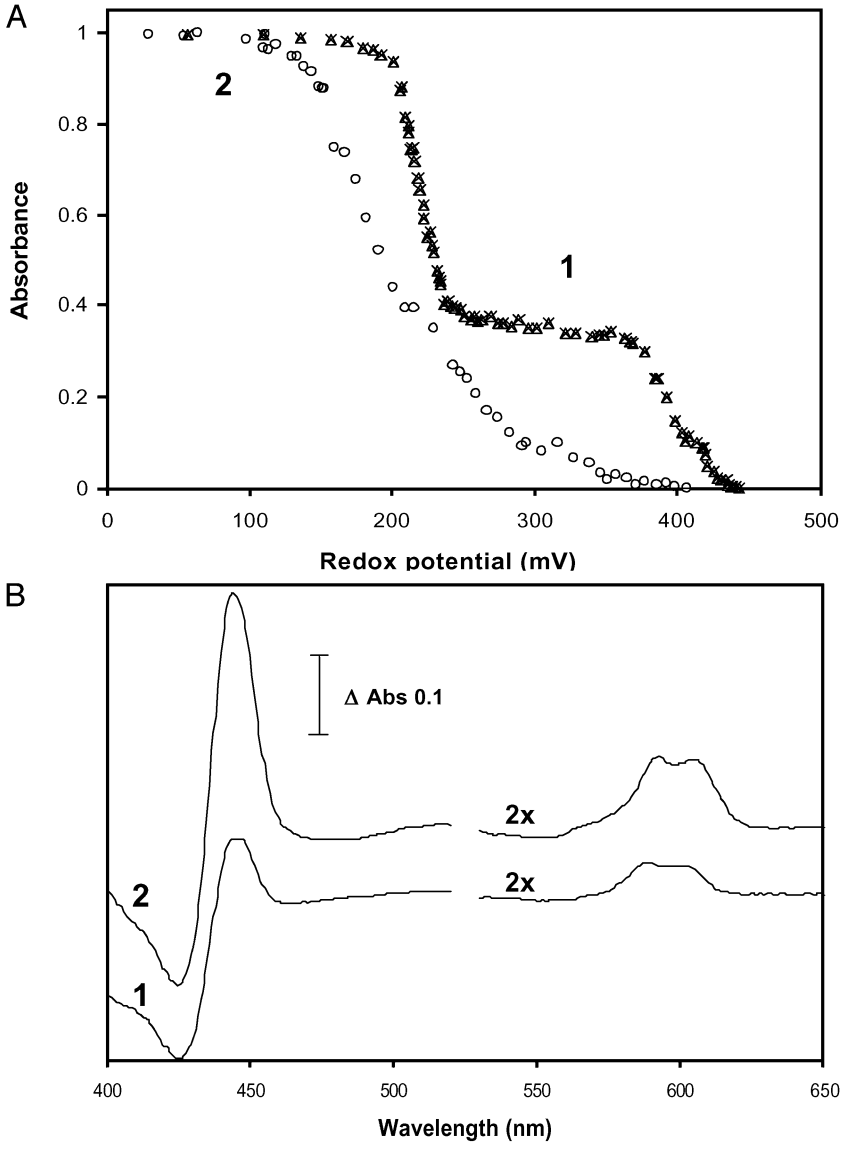

Fig. 6. Redox titration of *A. ambivalens* oxygen reductase at pH 7.5. Panel A: The reduction of the enzyme was followed at 604 nm for the pure enzyme (○) and at 592 nm (×) and 604 nm (△) for the cyanide-incubated enzyme. The absorbances are normalized in relation to the fully reduced enzyme. Panel B: The redox spectrum (reduced–oxidized) for the first (1) and second (2) redox transitions are shown.

oxygen reductase family varies, falling into two major groups corresponding to two conformers of the binuclear site. The first one, termed the α-conformer exhibits ν_{Fe-CO} at ~ 520 cm^{-1}; the second one, the β-conformer, has ν_{Fe-CO} at ~ 500 cm^{-1} [18,30]. Additionally, at alkaline pH, only one line at 493 cm^{-1} is seen in this region of the spectrum, the δ-conformer, which develops when the heme environment has been irreversibly disrupted. In the aa_3 oxygen reductase from *Rhodobacter sphaeroides*, the α- and β-conformers coexist and display a pH-dependent equilibrium [18,30]. Similar α- and β-conformers have been detected in the CO-bound forms of several other oxygen reductases from various organisms and have been studied by both FTIR and resonance Raman measurements [31–36].

The resonance Raman spectra of the CO derivative of *A. ambivalens* aa_3 in the low-frequency region are shown in Fig. 7. The lines at 500 and 520 cm^{-1} (spectrum b) are assigned as Fe–CO stretching modes, since in the $^{13}C^{18}O$ adduct (spectrum a, pH 7.4), the lines shift to 490 and 508 cm^{-1}, respectively, close to the expected isotope shifts for Fe–CO stretching modes. The Fe–C–O bending mode (δ_{Fe-C-O}), assigned at 567 cm^{-1}, shifts to 549 cm^{-1} with $^{13}C^{18}O$. It may be noted that the δ_{Fe-C-O} frequency in *A. ambivalens* appears at a much lower (11 cm^{-1}) frequency compared to that in the bovine enzyme (Table 1), suggesting that the bending characteristics of the Fe–C–O group are different in the two enzymes. The two Fe–CO stretching modes are assigned as originating from two different conformers (the 520 cm^{-1} line corresponds to the α-form and the 500 cm^{-1} line corresponds to the β-form) of the binuclear center, just as in *R. sphaeroides* aa_3 [30]. The two conformers do not exhibit any major change in their population (i.e. band intensity) in the pH range 5–9 (data not shown; only slight changes are seen in spectrum c at pH 9.0). At alkaline pH (~ 10.5), however, the enzyme has a single Fe–CO line at 494 cm^{-1}, with virtually no line at 567 cm^{-1}. This Fe–CO frequency at alkaline pH is assigned to a δ-conformer of the enzyme as reported for the *R. sphaeroides* aa_3 oxygen reductase [18]. Only one weak isotope-sensitive line was detected in the high-frequency region at 1970 cm^{-1} (spectra not shown) that we assign as a C–O stretching mode. Although we are unable to demonstrate which conformer it is associated with, we assume it is the α conformer as the ν_{C-O} frequency of this conformer is located at 1964 cm^{-1} in bovine and *R. sphaeroides* aa_3 (Table 1).

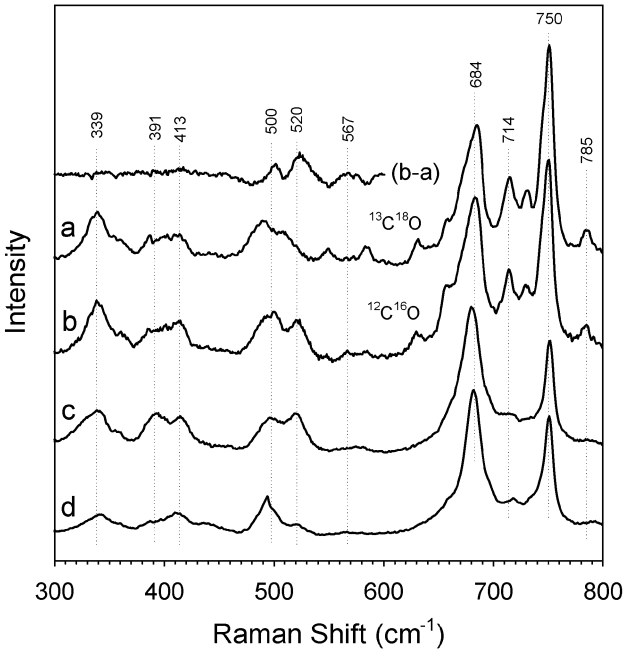

Fig. 7. Low-frequency resonance Raman spectra of the CO-derivative of aa_3 oxygen reductase of *A. ambivalens* as a function of pH and CO isotope. (a) pH 7.4, $^{13}C^{18}O$; (b) pH 7.4, $^{12}C^{16}O$; (c) pH 9.0, $^{12}C^{16}O$; and (d) pH 10.5, $^{12}C^{16}O$. The $^{12}C^{16}O$ minus $^{13}C^{18}O$ difference spectrum is shown at the top. Separate samples were made in the desired buffers for each pH value reported, and they were allowed to equilibrate following dithionite reduction as well as after CO addition. The laser excitation wavelength was 413.1 nm. The laser power used was 0.1–1.0 mW depending on the photoreducibility of the sample. Resonance Raman spectra of the CO samples prepared at pH 6 and pH 5 were very similar (not shown) to that for the pH 7.4 sample.

The two CO conformations are proposed to originate from a difference in their a_3Fe-Cu_B distance [18]. Although Fe–CO and C–O frequencies of most hemeproteins follow an inverse correlation, those of the α-conformer of the oxygen reductases lie off the Fe–CO vs. the C–O correlation curve [37]. The assignment of the C–O frequency at 1970 cm^{-1} and the Fe–CO frequency at 520 cm^{-1} for the α-conformer of *A. ambivalens* places it off the correlation curve just as in the other oxygen reductases. The C–O frequency of the β-conformer in the *A. ambivalens* enzyme is not detected in this work. It may be noted that the β-conformer in the *R. sphaeroides* enzyme has been shown to lie on the correlation line [18] unlike the α-conformer. It is likely that due to the steric constraints in the binuclear center resulting from Cu_B, in the α-conformer, the Fe–C–O moiety is significantly bent and possibly the Fe–C bond is compressed.

In bovine aa_3, incubation of the enzyme with CO leads first to the mixed valence species and later to the fully reduced species [38]. However, unlike the bovine enzyme, the yield of a CO-induced mixed valence species is very low in the *A. ambivalens* enzyme as may be seen in Fig. 5, spectrum e. For comparison, the spectrum of the fully reduced CO-bound enzyme is shown in spectrum f.

3.6. The alkaline transition in oxidized *A. ambivalens* aa_3 oxygen reductase

Although *A. ambivalens* aa_3 remains active (and structurally stable) over a wider acidic pH range than the bovine enzyme, it is less stable in the alkaline pH range. As low as at pH 9, the enzyme displays significant changes in the structure of its redox cofactors. Raman spectra of the oxidized form of the *A. ambivalens*

enzyme at three alkaline pHs are shown in Fig. 8. The spectra at high pH are similar to those reported by Babcock et al. [21] on the mammalian enzyme. Two important changes occur in these spectra at the elevated pH: the ν_3 mode at $\sim$ 1490 cm^{-1} becomes very strong and two broad lines are present in the high-frequency region at 1580 and 1625–1635 cm^{-1}. The frequency of the ν_3 mode is characteristic of five-coordinate high-spin ferric hemes, and its intensity, which is comparable to that of the ν_4 mode at 1370–1375 cm^{-1}, is similar to that seen in model complexes [39], mutant myoglobins [40], heme oxygenase [41], and bovine aa_3 (H. Ji, S.-R. Yeh, D.L. Rousseau, unpublished results) under conditions in which the heme is coordinated by a hydroxide ion. We postulate that in the alkaline form of the *A. ambivalens* enzyme a hydroxide group serves as the fifth ligand of the heme and that the proximal histidine–iron bond is broken. However, no Fe–OH stretching mode in alkaline *A. ambivalens* enzyme could be detected in experiments conducted with $H_2O/D_2O/H_2^{18}O$ in the low-frequency region, probably because the Fe–OH mode is very weak.

Broad lines at higher frequency (1580 and $\sim$ 1630 cm^{-1}) are characteristic of Schiff base formation of the heme formyl groups [42,43] (H. Ji, S.-R. Yeh, D. L. Rousseau, unpublished results), which was confirmed by the observation of the C=N stretching mode in the bovine enzyme [42]. Thus, we conclude that under these alkaline conditions in the *A. ambivalens* oxygen reductase, a Schiff base has been formed. We propose that the histidine–iron bonds for both heme *a* and heme a_3 have been broken allowing the hemes to move out of their pockets. Similar results have been found in the bovine enzyme but this enzyme is stable up to pH $\sim$ 10, and the Schiff base is formed at pH $\sim$ 11 and higher [21]. Thus, the onset of alkaline transition in *A. ambivalens* aa_3 occurs at a much lower pH than in the bovine enzyme, while the *A. ambivalens* enzyme exhibits more acid tolerance. Apparently, such structural and functional properties of the *A. ambivalens* enzyme befit well the living conditions of this extremophile that is known to thrive at an acid pH of 2.5, although the internal cellular pH may be much higher.

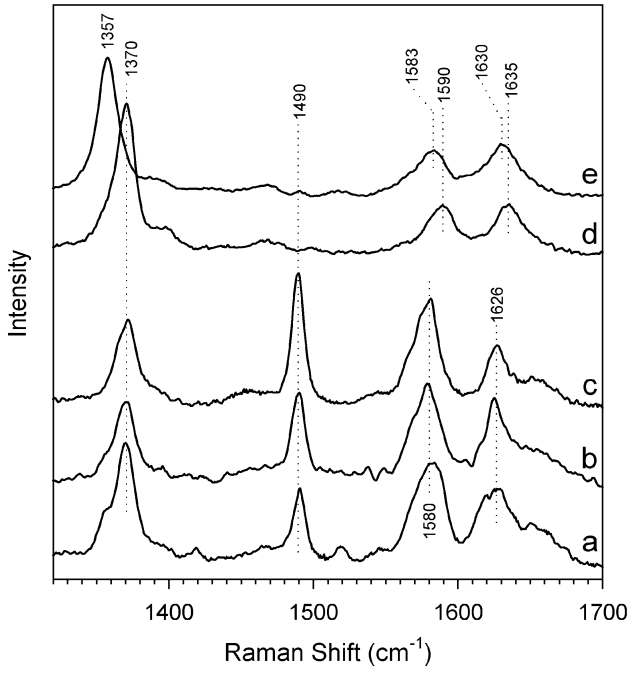

Fig. 8. Resonance Raman spectra of alkaline *A. ambivalens* aa_3 oxygen reductase in the oxidized and reduced states in the high-frequency region. The spectra of the oxidized enzyme shown are at (a) pH 9; (b) pH 9.5; (c) pH 10.5. Also shown are spectra of (d) dithionite-reduced CO-bound species, pH 10.5, and (e) dithionite-reduced species, pH 10.5. The excitation frequency was 413.1 nm, and laser power used on the sample was 0.5–2 mW.

3.7. The effect of low pH and photolysis

The resonance Raman spectra of hemeproteins in their ferrous oxidation state (with a five-coordinated heme ligated to a histidine) generally have a low-frequency line in the neighborhood of 220 cm^{-1} resulting from the Fe–His stretching mode (ν_{Fe-His}). This mode is sensitive to strain in the Fe–His bond and the electrostatic environment of the histidine, and thus it is a useful probe to study the structural dynamics of the heme pocket [44,45]. The ν_{Fe-His} mode in *A. ambivalens* aa_3 is assigned at 210 cm^{-1} in the reduced enzyme (Fig. 9, bottom, spectrum a), by similarity with that in other aa_3 oxygen reductases. As shown in Fig. 9 (spectra a–c), the majority of the lines of the reduced enzyme in the low-frequency region spectrum do not show any significant changes as a function of pH. Even at pH 2.6, the spectrum is very similar to that at neutral pH, except for a decrease in the intensity of the line at 329 cm^{-1} and a shift in the ν_{Fe-His} line to 207 cm^{-1} with a concomitant decrease in its intensity. The presence of the Fe–His mode in the spectrum at pH 2.6 is a surprising result as the pK_a for histidine is $\sim$ 6.0, although in proteins its pK_a can vary substantially. Thus, at pH 2.6, it would be expected that the histidine would become protonated and so the Fe–His bond would not be maintained. Apparently, the access to the heme site by the protons is limited, thereby allowing the Fe–His bond to remain intact.

The frequency of the Fe–His stretching mode in *A. ambivalens* is lower than that in most heme proteins. Model compound and other heme protein studies have demonstrated that a low frequency results from strain on the Fe–His bond and/or the absence of H-bonding to the δ nitrogen atom of the histidine. A way to distinguish the two effects is to do a photolysis experiment. For example, in hemoglobin, the Fe–His stretching mode is located at 214 cm^{-1} under equilibrium conditions [46]. However, upon CO photolysis, it shifts to 230 cm^{-1} [46]. This is a consequence of the strain being alleviated in the CO-bound form, so upon

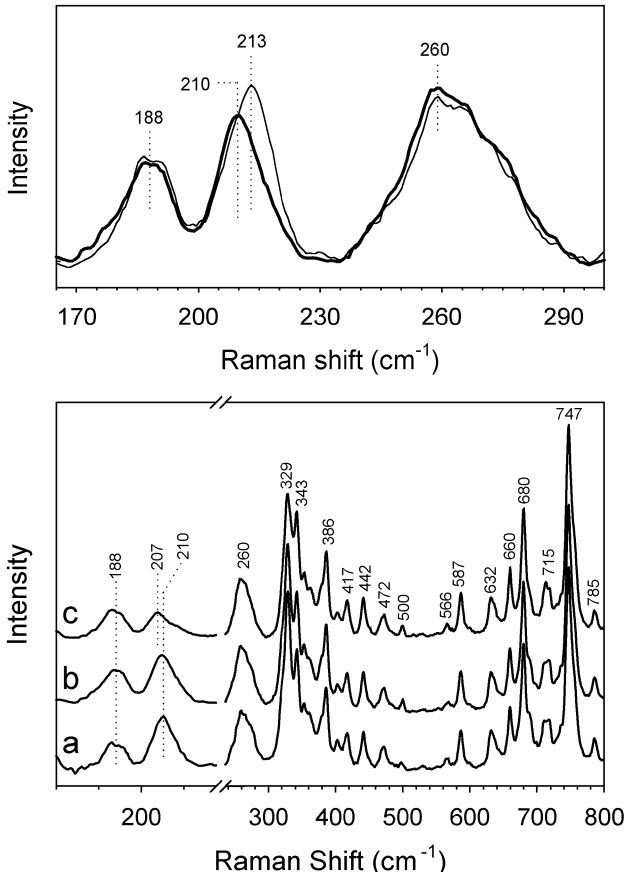

Fig. 9. Resonance Raman spectra of reduced *A. ambivalens* aa_3 oxygen reductase in the low-frequency region. Bottom, dithionite-reduced enzyme at (a) pH 7.4, (b) pH 6, and (c) pH 2.6. Top, dithionite-reduced enzyme (bold line) and CO-photodissociated enzyme (thin line), both at pH 6. Excitation frequency was 441.7 nm, and the laser power at sample was $\sim$ 20 mW. The purified enzyme (60 μM) was reduced anaerobically by dithionite, in 100 mM MES and 1 mg/ml dodecyl maltoside at pH 6.0. To prepare the CO complex, the dithionite-reduced enzyme was exposed to CO under anaerobic conditions. The CO complex was photodissociated and probed by the 441.7 nm beam in the rotating cell under conditions such that the time evolution of the photoproduct was $\sim$ 2 μs.

photolysis before protein relaxation, the frequency of the photodissociated species reflects the structure in the absence of strain. For the bovine enzyme the Fe–His mode shifted from 213 to 219 cm^{-1} upon photolysis at 10 ns [47]. In *A. ambivalens*, the relaxed frequency is even lower (210 cm^{-1}) than in the bovine enzyme and the photolysis at $\sim$ 2 μs only shifts the frequency by 3 cm^{-1} (see Fig. 9, top). Therefore, the low frequency of the mode is not fully alleviated by the photolysis, indicating that the frequency of the mode does not result from a highly strained bond. Instead, the low frequency appears to be a consequence of the N_δ environment.

The proximal histidine (His-376) of heme a_3 in the bovine enzyme forms a hydrogen bond to the backbone carbonyl of Gly-351 [12]. Apparently, this hydrogen bond is weak, resulting in the low frequency for the Fe–His mode ($\sim$ 213 cm^{-1}). When the H bond is very strong resulting in a higher degree of deprotonation of the histidine N_δ, such as in the case of peroxidases, the frequency of the Fe–His stretching mode is very high [48]. A lower frequency of the ν_{Fe-His} frequency at 210 cm^{-1} in *A. ambivalens* suggests that the effective occupancy of proton at N_δ is further increased, implying that the hydrogen bond of the proximal histidine (tentatively His-379) with a residue (tentatively Ala-354, which may be the equivalent of Gly-351 in bovine enzyme, on the basis of sequence similarity analysis) is weaker than in the bovine enzyme. No shift in ν_{Fe-His} in the H_2O vs. D_2O comparison (data not shown) was detected, possibly due the lack of accessibility of solvents to the heme a_3 proximal pocket as reported previously [49]. The difference in the frequency of the Fe–His stretching mode in *A. ambivalens* as compared to the bovine enzyme could have a great deal of functional significance as it was recently postulated that differences in the level of the H bonding of the proximal histidine could be involved in defining the difference between the structures of the "P" and "F" intermediates [50].

4. Discussion

A. ambivalens is a hyperthermoacidophilic archaeon that grows optimally at 80 °C and pH 2.5 [6,7]. In its simple respiratory system, it contains a cytochrome aa_3 quinol:oxygen oxidoreductase that is a member of the superfamily of heme–copper oxygen reductases and like the other members it has been shown to pump protons [5]. Given that the organism functions under extreme conditions, and that the enzyme belongs to the B-type subgroup of the heme–copper superfamily [1,2], it might be expected that the properties of *A. ambivalens* aa_3 would have some significant differences in comparison to the canonical members of the family. The results obtained here demonstrate that the protein shares some of the common features with the other members of the family and also has some distinct properties.

4.1. Heme a environment

One of the characteristic properties of the heme *a* environment is the frequency of the carbonyl stretching mode of the formyl group. In the bovine enzyme, this mode is located at 1611 cm^{-1} in the reduced enzyme and at 1647 cm^{-1} in the oxidized enzyme. This change has been interpreted as being due to a large change in the strength of the hydrogen bonding to the formyl group, being very strong in the reduced enzyme and weakened in the oxidized form [21]. In contrast, in the terminal aa_3 oxygen reductase from another extremophilic organism, *S. acidocaldarius*, which also grows at low pH and high temperature, there is no change in the frequency of the formyl mode upon changing the oxidation state [25]. Instead, the mode is assigned at $\sim$ 1656 cm^{-1} in both redox states, suggesting that the formyl group is in a rather hydrophobic environ-

ment in both states [25]. In the data reported here from *A. ambivalens*, a significant shift in the frequency is detected upon oxidation (1629–1653 cm^{-1}), although it is somewhat smaller than that in the bovine enzyme, because the frequency of the mode in the reduced state is higher. Thus, the environment of the heme *a* near the formyl group is similar in the bovine, *A. ambivalens*, and *S. acidocaldarius* enzymes in the oxidized state but very different in the reduced state, ranging from very strong to very weak hydrogen bonding, respectively.

The change in strength of the H bond between the oxidized and reduced states among these three oxidases suggests that it is not a functionally important parameter that affects the overall oxygen reduction or proton pumping. However, the environment may have an effect on the midpoint potentials and thereby affect the electron transfer processes and ultimately the rates of the functional processes. Indeed, it has been found that the midpoint potentials of the hemes in *A. ambivalens* are very different from those in the bovine enzyme. In the bovine enzyme, heme *a* has a higher potential than that of heme a_3 (in the absence of heme–heme interaction), whereas in the *A. ambivalens* oxidase, heme a_3 has a higher midpoint potential [4]. This difference is also consistent with the rates of reduction of the hemes by the addition of dithionite [4]. This switching of the relative potentials appears to be a consequence of both the heme *a* potential being lower and the heme a_3 potential being higher in the *A. ambivalens* oxygen reductase as compared to the corresponding potentials in the bovine enzyme. However, it is recognized that there are likely to be heme–heme redox interactions in *A. ambivalens*, just as in the mammalian enzyme, that alters the potentials under partially reduced conditions.

4.2. The proximal side of heme a_3

The Fe–His stretching mode serves as a probe of the environment on the proximal side of ferrous five-coordinate heme groups [46,51]. The frequency of this mode in the *A. ambivalens* enzyme is slightly lower than that of the bovine enzyme, suggesting that the environment near the histidine is less polar than in the bovine case. The absence of a large increase in frequency of the mode upon CO photolysis demonstrates that this low frequency is a consequence of the nonpolar environment and not of strain in the Fe–His bond. In addition, the absence of any changes detectable in the mode upon changing from protonated to deuterated buffers and the presence of the line at very low pH conditions indicates that access to this region by protons is very limited. The lack of the free access could have important consequences for proton translocation properties in that there would not be expected to be any leakage of protons that could deplete the proton gradient.

In contrast to the stability of the protein under low pH conditions, the *A. ambivalens* enzyme is less stable than the bovine oxidase at high pH. The conversion from the native structure to a five-coordinate hydroxide-bound species with Schiff base formation of the formyl groups of both hemes is detectable at pH 9. We postulate that for this to happen, the protein has become destabilized such that the hemes have become exposed. The instability of the protein at high pH in contrast to its high stability at low pH is compatible with the environmental conditions of *A. ambivalens* that thrives only at low pH.

4.3. The catalytic binding site

To probe the properties of the catalytic site, the carbon monoxide and the cyanide adducts were studied. Exogenous ligands serve as useful probes of the catalytic site because they are sensitive to the local interactions that are related to the types of interactions that occur in the oxy complexes and the associated redox intermediates. The CO adducts of many heme proteins have been studied and the Fe–C–O modes have been especially useful in the determination of heme pocket interactions. In the canonical oxygen reductases, the negative correlation between the Fe–CO mode and the C–O modes of the heme a_3 species lie in a unique position with respect to other heme proteins, in that they do not fall on the correlation curve for the histidine–Fe–CO complex [30,33]. Recently, a great deal of useful information concerning the properties of the catalytic site in several different oxygen reductases have been obtained by a combination of resonance Raman and FTIR studies of CO complexes by Varotsis et al. [33–36]. One of their important findings was that the Cu_B–CO complexes are quite robust. In particular, they found that this complex in the ba_3 oxygen reductase from *Thermus thermophilus* is insensitive to pH over the 5.5 to 9.7 range and concluded that the Cu_B histidine ligands did not undergo any protonation/deprotonation events [35] as postulated in several models for proton pumping [8,52,53]. However, changes in the electrostatic properties of the binuclear center during the oxygen reduction process could bring about changes in the histidine protonation and/or ligation states that may be essential elements of proton translocation pathways, but such changes may not occur in the CO complex.

In *A. ambivalens* aa_3, there are two Fe–CO modes present in the spectrum. These have been assigned as being associated with the α and β forms of the protein as has been seen in other oxygen reductases [18,30–36]. In addition, Fe–C–O modes of one form (the α-form) lie off the Fe–CO vs. the C–O correlation curve just as in the other enzymes. The failure to lie on the curve in other oxidases has been attributed to interactions between the CO and the Cu_B atom [18] that has been found to be only 5 Å from the heme iron atom [12]. This confirms that the heme interactions in *A. ambivalens* aa_3 are the same as those in the other members of the heme–copper oxygen reductase superfamily.

In the bovine aa_3 oxygen reductase, the addition of CO to the resting enzyme leads to a mixed valence state in a

period of a few hours or less [54]. The mechanism for this process involves the oxidation of CO to CO_2 and requires a molecule of water; that is

$$Cu^{2+}Fe^{3+} + CO + H_2O \rightarrow Cu^{1+}Fe^{2+} + CO_2 + 2H^+$$

It has been reported that the process is dependent on the presence of hydroxide ions and has been found to occur in other heme proteins but at a much slower rate [54]. The observation that this does not occur in *A. ambivalens* aa_3 is at first a surprising result since the midpoint potential of the heme a_3 is high [4]; thus, one would expect that it would be readily reduced. If the mechanism involves the formation of a stable hydroxyl species as is likely the case, then a high midpoint potential may not be critical. Instead, the formation of a stable hydroxide-bound heme associated with certain electrostatic features of the heme pocket may be the critical elements needed for the reduction. The cyanide results in which the same level of stability is not achieved in the *A. ambivalens* as in the bovine enzyme suggests that the electrostatics of the heme pocket are not the same in the two enzymes and negatively charged ligands such as the hydroxide are not as readily stabilized in *A. ambivalens* at physiological pH.

The spectral properties and the redox titration of the heme a_3 cyanide adduct confirms that the midpoint potentials are very different from those of the bovine enzyme. In the bovine enzyme, the cyanide adduct forms a very stable complex with the oxidized enzyme that is very hard to reduce. Thus, it readily forms a mixed valence species in which the heme *a* is reduced and the CN-bound heme a_3 is oxidized. For *A. ambivalens*, the CN adduct can be readily reduced and no mixed valence species is formed. Analysis of the redox titration data demonstrates that there is extensive heme–heme interaction of the cyanide adduct such that the data can only be accounted for by the neoclassical model [55]. This difference in the apparent electrostatic environment of the cyanide-bound enzyme suggests that the stabilization of the catalytic intermediates may be quite different in *A. ambivalens* as compared to the bovine enzyme and, thus, a thorough study of the catalytic process is warranted.

4.4. Proton pumping

One of the most remarkable features of the spectroscopic properties of the aa_3 oxygen reductase from *A. ambivalens* is the slow change in the frequency of the carbonyl stretching mode of the formyl group of heme a_3 upon reduction. This change has been interpreted as the gradual loss of H bonding to the carbonyl group and is thereby evidence for a slow conformational change in the heme environment. Based on this change in the protonation of the formyl group, we previously proposed a mechanism for proton translocation [8]. This model for proton translocation was based on the premise that the overall structure of the oxygen reductase from *A. ambivalens* is the same as those of the reported mammalian and bacterial enzymes. Within this limitation, the only residue close enough to the formyl group capable of transient H-bonding would be His-290, one of the Cu_B ligands, and thus, the position and/or the protonation state of His-290 could be electrostatically controlled by charges in the catalytic site during the redox process. Its conformational changes could regulate the release of protons and thus be the central element in the redox-coupled proton translocation. In this model, the formyl group serves as an H bond acceptor, but the central element of the mechanism is the protonation state of His-290.

It has been established that the enzyme from *A. ambivalens* is a proton pump, but the channels through which the protons pass are not the same as those in the bovine or the mitochondrial-like enzymes that have been studied [5]. In addition, the caldariella quinone, which is thought to be tightly bound to the enzyme in vivo, affects the electron transport properties and the structural properties around the hemes [4]. Thus, while there are many similarities between the *A. ambivalens* oxygen reductase and those from other species, as pointed out here and elsewhere, there are many differences, which may be characteristic of the B-type family to which the *A. ambivalens* enzyme belongs [2]. Consequently, while the general principles of the proton pumping mechanism may be the same, the specific elements involved or their organization may result from a fine tuning that the members of the different families of oxygen reductases have acquired throughout evolution. On this basis, the mechanism that was proposed may be valid for the *A. ambivalens* oxygen reductase but may have structural differences in comparison to other enzymes. Thus, a redox-linked control of the protonation state of a residue in the catalytic site, such as His-290, may be a central element of all proton pumps but the specific residue that plays that role may differ especially when comparing very diverse oxygen reductases.

Acknowledgements

This work was supported in part by grant POCTI Bio36560/99 to MT and by National Institutes of Health Grant GM54806 to DLR. CGM acknowledges the Fundação Calouste Gulbenkian (Programa Estímulo à Investigação). TB and MMP are recipients of grants from PRAXIS XXI Program (BD/3133/00 and BPD/22054/99). We thank Ms. Hong Ji and Dr. Syun-Ru Yeh of Albert Einstein College of Medicine and Dr. Alessandro Giuffrè of the University of Rome for stimulating discussions.

References

[1] M.M. Pereira, M. Santana, M. Teixeira, A novel scenario for the evolution of haem–copper oxygen reductases, Biochim. Biophys. Acta 1505 (2001) 185–208.

[2] M.M. Pereira, C.M. Gomes, M. Teixeira, Plasticity of proton pathways in haem–copper oxygen reductases, FEBS Lett. 522 (2002) 14–18.
[3] S. Anemuller, C.L. Schmidt, I. Pacheco, G. Schafer, M. Teixeira, A cytochrome aa_3-type quinol oxidase from *Desulfurolobus ambivalens*, the most acidophilic archaeon, FEMS Microbiol. Lett. 117 (1994) 275–280.
[4] A. Giuffre, C.M. Gomes, G. Antonini, E. D'Itri, M. Teixeira, M. Brunori, Functional properties of the quinol oxidase from *Acidianus ambivalens* and the possible catalytic role of its electron donor–studies on the membrane-integrated and purified enzyme, Eur. J. Biochem. 250 (1997) 383–388.
[5] C.M. Gomes, C. Backgren, M. Teixeira, A. Puustinen, M.L. Verkhovskaya, M. Wikstrom, M.I. Verkhovsky, Heme–copper oxidases with modified D- and K-pathways are yet efficient proton pumps, FEBS Lett. 497 (2001) 159–164.
[6] T. Fuchs, H. Huber, S. Burggraf, K.O. Stetter, Syst. Appl. Microbiol. 19 (1996) 56–60.
[7] W. Zillig, S. Yeats, I. Holz, A. Bock, F. Gropp, M. Rettenberger, S. Lutz, Plasmid-related anaerobic autotrophy of the novel archaebacterium *Sulfolobus ambivalens*, Nature 313 (1985) 789–791.
[8] T.K. Das, C.M. Gomes, M. Teixeira, D.L. Rousseau, Redox-linked transient deprotonation at the binuclear site in the *aa*(3)-type quinol oxidase from *Acidianus ambivalens*: implications for proton translocation, Proc. Natl. Acad. Sci. U. S. A. 96 (1999) 9591–9596.
[9] A. Aagaard, G. Gilderson, C.M. Gomes, M. Teixeira, P. Brzezinski, Dynamics of the binuclear center of the quinol oxidase from *Acidianus ambivalens*, Biochemistry 38 (1999) 10032–10041.
[10] A. Puustinen, M.I. Verkhovsky, J.E. Morgan, N.P. Belevich, M. Wikstrom, Reaction of the *Escherichia coli* quinol oxidase cytochrome bo_3 with dioxygen: the role of a bound ubiquinone molecule, Proc. Natl. Acad. Sci. U. S. A. 93 (1996) 1545–1548.
[11] J. Behr, P. Hellwig, W. Mantele, H. Michel, Redox dependent changes at the heme propionates in cytochrome *c* oxidase from *Paracoccus denitrificans*: direct evidence from FTIR difference spectroscopy in combination with heme propionate ^{13}C labeling, Biochemistry 37 (1998) 7400–7406.
[12] S. Yoshikawa, K. Shinzawa-Itoh, R. Nakashima, R. Yaono, E. Yamashita, N. Inoue, M. Yao, M.J. Fei, C.P. Libeu, T. Mizushima, H. Yamaguchi, T. Tomizaki, T. Tsukihara, Redox-coupled crystal structural changes in bovine heart cytochrome *c* oxidase, Science 280 (1998) 1723–1729.
[13] T.K. Das, S. Mazumdar, Conformational change due to reduction of cytochrome-*c* oxidase in lauryl maltoside: picosecond time-resolved tryptophan fluorescence studies on the native and heat modified enzyme, Biochim. Biophys. Acta 1209 (1994) 227–237.
[14] J.P. Osborne, N.J. Cosper, C.M. Stalhandske, R.A. Scott, J.O. Alben, R.B. Gennis, Cu XAS shows a change in the ligation of CuB upon reduction of cytochrome bo3 from *Escherichia coli*, Biochemistry 38 (1999) 4526–4532.
[15] M. Ralle, M.L. Verkhovskaya, J.E. Morgan, M.I. Verkhovsky, M. Wikstrom, N.J. Blackburn, Coordination of CuB in reduced and CO-liganded states of cytochrome bo3 from *Escherichia coli*. Is chloride ion a cofactor? Biochemistry 38 (1999) 7185–7194.
[16] P. Wittung, B.G. Malmstrom, Redox-linked conformational changes in cytochrome *c* oxidase, FEBS Lett. 388 (1996) 47–49.
[17] M. Teixeira, R. Batista, A.P. Campos, C. Gomes, J. Mendes, I. Pacheco, S. Anemuller, W.R. Hagen, A seven-iron ferredoxin from the thermoacidophilic archaeon *Desulfurolobus ambivalens*, Eur. J. Biochem. 227 (1995) 322–327.
[18] T.K. Das, F.L. Tomson, R.B. Gennis, M. Gordon, D.L. Rousseau, pH-dependent structural changes at the Heme–Copper binuclear center of cytochrome *c* oxidase, Biophys. J. 80 (2001) 2039–2045.
[19] M.M. Pereira, J.N. Carita, M. Teixeira, Membrane-bound electron transfer chain of the thermohalophilic bacterium *Rhodothermus marinus*: characterization of the iron–sulfur centers from the dehydrogenases and investigation of the high-potential iron–sulfur protein function by in vitro reconstitution of the respiratory chain, Biochemistry 38 (1999) 1276–1283.
[20] T.G. Spiro, J.M. Burke, Protein control of porphyrin conformation. Comparison of resonance Raman spectra of heme proteins with mesoporphyrin IX analogues, J. Am. Chem. Soc. 98 (1976) 5482–5489.
[21] P.M. Callahan, G.T. Babcock, Origin of the cytochrome a absorption red shift: a pH-dependent interaction between its heme a formyl and protein in cytochrome oxidase, Biochemistry 22 (1983) 452–461.
[22] P.V. Argade, Y.C. Ching, D.L. Rousseau, Cytochrome a_3 structure in carbon monoxide-bound cytochrome oxidase, Science 225 (1984) 329–331.
[23] P.V. Argade, Y.C. Ching, D.L. Rousseau, Resonance Raman spectral isolation of the *a* and a_3 chromophores in cytochrome oxidase, Biophys. J. 50 (1986) 613–620.
[24] Y.C. Ching, P.V. Argade, D.L. Rousseau, Resonance Raman spectra of CN-bound cytochrome oxidase: spectral isolation of cytochromes *a*2+, *a*3(2+), and *a*3(2+)(CN −), Biochemistry 24 (1985) 4938–4946.
[25] G.E. Heibel, P. Anzenbacher, P. Hildebrandt, G. Schafer, Unusual heme structure in cytochrome aa3 from *Sulfolobus acidocaldarius*: a resonance Raman investigation, Biochemistry 32 (1993) 10878–10884.
[26] K.J. van Buuren, P. Nicholis, B.F. van Gelder, Biochemical and biophysical studies on cytochrome aa_3: VI. Reaction of cyanide with oxidized and reduced enzyme, Biochim. Biophys. Acta 256 (1972) 258–276.
[27] M.K. Johnson, D.G. Eglinton, P.E. Gooding, C. Greenwood, A.J. Thomson, Characterization of the partially reduced cyanide-inhibited derivative of cytochrome *c* oxidase by optical, electron-paramagnetic-resonance and magnetic-circular-dichroism spectroscopy, Biochem. J. 193 (1981) 699–708.
[28] A.J. Moody, C.E. Cooper, P.R. Rich, Characterisation of 'fast' and 'slow' forms of bovine heart cytochrome-*c* oxidase, Biochim. Biophys. Acta 1059 (1991) 189–207.
[29] P.G. Papadopoulos, S.A. Walter, J.W. Li, G.M. Baker, Proton interactions in the resting form of cytochrome oxidase, Biochemistry 30 (1991) 840–850.
[30] J. Wang, S. Takahashi, J.P. Hosler, D.M. Mitchell, S. Ferguson-Miller, R.B. Gennis, D.L. Rousseau, Two conformations of the catalytic site in the *aa*3-type cytochrome *c* oxidase from *Rhodobacter sphaeroides*, Biochemistry 34 (1995) 9819–9825.
[31] J. Wang, Y.-C. Ching, D.L. Rousseau, J.J. Hill, J. Rumbley, R.B. Gennis, Similar CO binding sites in bacterial cytochrome *bo* and mammalian cytochrome *c* oxidase, J. Am. Chem. Soc. 115 (1993) 3390–3391.
[32] J. Wang, K.A. Gray, F. Daldal, D.L. Rousseau, The cbb_3-type cytochrome *c* oxidase from *Rhodobacter capsulatus* contains a unique active site, J. Am. Chem. Soc. 117 (1995) 9363–9364.
[33] E. Pinakoulaki, T. Soulimane, C. Varotsis, Fourier transform infrared (FTIR) and step-scan time-resolved FTIR spectroscopies reveal a unique active site in cytochrome *c*aa3 oxidase from *Thermus thermophilus*, J. Biol. Chem. 277 (2002) 32867–32874.
[34] E. Pinakoulaki, U. Pfitzner, B. Ludwig, C. Varotsis, The role of the cross-link His–Tyr in the functional properties of the binuclear center in cytochrome *c* oxidase, J. Biol. Chem. 277 (2002) 13563–13568.
[35] K. Koutsoupakis, S. Stavrakis, E. Pinakoulaki, T. Soulimane, C. Varotsis, Observation of the equilibrium CuB–CO complex and functional implications of the transient heme a_3 propionates in cytochrome ba_3–CO from *Thermus thermophilus*. Fourier transform infrared (FTIR) and time-resolved step-scan FTIR studies, J. Biol. Chem. 277 (2002) 32860–32866.
[36] K. Koutsoupakis, S. Stavrakis, T. Soulimane, C. Varotsis, Oxygen-linked equilibrium CuB–CO species in cytochrome ba_3 oxidase from *thermus thermophilus*. Implications for an oxygen channel ar the CuB site, J. Biol. Chem. 278 (2003) 14893–14896.
[37] N.T. Yu, E.A. Kerr, in: T.G. Spiro (Ed.), Biological Applications of Raman Spectroscopy, Resonance Raman Spectra of Heme and Metalloproteins, vol. 3, Wiley, New York, 1988, pp. 39–95.
[38] C. Greenwood, M.T. Wilson, M. Brunori, Studies on partially reduced

mammalian cytochrome oxidase: reactions with carbon monoxide and oxygen, Biochem. J. 137 (1974) 205–215.
[39] A. Boffi, T.K. Das, S. della Longa, C. Spagnuolo, D.L. Rousseau, Pentacoordinate hemin derivatives in sodium dodecyl sulfate micelles: model systems for the assignment of the fifth ligand in ferric heme proteins, Biophys. J. 77 (1999) 1143–1149.
[40] T.K. Das, S. Franzen, A. Pond, J.H. Dawson, D.L. Rousseau, Formation of a five-coordinate hydroxide-bound heme in the His93Gly mutant of sperm whale myoglobin, Inorg. Chem. 38 (1999) 1952–1953.
[41] G.C. Chu, M. Couture, T. Yoshida, D.L. Rousseau, M. Ikeda-Saito, Axial ligation states of five-coordinate heme oxygenase proximal histidine mutants as revealed by EPR and resonance Raman spectroscopy, J. Am. Chem. Soc. 122 (2000) 12612–12613.
[42] S.W. Han, Y.C. Ching, S.L. Hammes, D.L. Rousseau, Vibrational structure of the formyl group on heme *a*. Implications on the properties of cytochrome *c* oxidase, Biophys. J. 60 (1991) 45–52.
[43] G.T. Babcock, I. Salmeen, Resonance Raman spectra and optical properties of oxidized cytochrome oxidase, Biochemistry 18 (1979) 2493–2498.
[44] O. Einarsdottir, R.B. Dyer, D.D. Lemon, P.M. Killough, S.M. Hubig, S.J. Atherton, J.J. Lopez-Garriga, G. Palmer, W.H. Woodruff, Photodissociation and recombination of carbonmonoxy cytochrome oxidase: dynamics from picoseconds to kiloseconds, Biochemistry 32 (1993) 12013–12024.
[45] J.P.M. Schelvis, G. Deinum, C.A. Varotsis, S. Ferguson-Miller, G.T. Babcock, Low-power picosecond resonance Raman evidence for histidine ligation to heme a_3 after photodissociation of CO from cytochrome *c* oxidase, J. Am. Chem. Soc. 119 (1997) 8409–8416.
[46] D.L. Rousseau, J.M. Friedman, in: T.G. Spiro (Ed.), Biological Applications of Raman Spectroscopy, Resonance Raman Spectra of Heme and Metalloproteins, vol. 3, Wiley, New York, 1988.
[47] M. Sassaroli, Y.C. Ching, P.V. Argade, D.L. Rousseau, Photodissociated cytochrome *c* oxidase: cryotrapped metastable intermediates, Biochemistry 27 (1988) 2496–2502.
[48] S. Dasgupta, D.L. Rousseau, H. Anni, T. Yonetani, Structural characterization of cytochrome *c* peroxidase by resonance Raman scattering, J. Biol. Chem. 264 (1989) 654–662.
[49] P.V. Argade, Y.C. Ching, M. Sassaroli, D.L. Rousseau, Accessibility of the cytochrome a heme in cytochrome *c* oxidase to exchangeable protons, J. Biol. Chem. 261 (1986) 5969–5973.
[50] E. Pinakoulaki, U. Pfitzner, B. Ludwig, C. Varotsis, Direct detection of Fe(IV)[double bond]O intermediates in the cytochrome aa_3 oxidase from *Paracoccus denitrificans*/H_2O_2 reaction, J. Biol. Chem. 278 (2003) 18761–18766.
[51] T. Kitagawa, in: T.G. Spiro (Ed.), Biological Applications of Raman Spectroscopy, Resonance Raman Spectra of Heme and Metalloproteins, vol. 3, Wiley, New York, 1988, pp. 97–131.
[52] J.E. Morgan, M.I. Verkhovsky, M. Wikstrom, The histidine cycle: a new model for proton translocation in the respiratory heme–copper oxidases, J. Bioenerg. Biomembranes 26 (1994) 599–608.
[53] S. Iwata, C. Ostermeier, B. Ludwig, H. Michel, Structure at 2.8 Å resolution of cytochrome *c* oxidase from *Paracoccus denitrificans*, [see comments], Nature 376 (1995) 660–669.
[54] D. Bickar, C. Bonaventura, J. Bonaventura, Carbon monoxide-driven reduction of ferric heme and heme proteins, J. Biol. Chem. 259 (1984) 10777–10783.
[55] P. Nicholis, J.M. Wrigglesworth, in: M. Brunori, B. Chance (Eds.), Cytochrome Oxidase: Structure, Function and Physiopathology, vol. 550, The New York Academy of Sciences, New York, 1988, pp. 59–67.